GRK2–YAP signaling is implicated in pulmonary arterial hypertension development

Peng Ye[1], Yunfei Deng[2,3], Yue Gu[2], Pengfei Liu[1], Jie Luo[2], Jiangqin Pu[1], Jingyu Chen[4], Yu Huang[5], Nanping Wang[6], Yong Ji[7], Shaoliang Chen[7,8]

[1]Division of Cardiovascular Molecular Laboratory, Third Clinical College, Nanjing Medical University, Nanjing, Jiangsu 210006, China;
[2]Division of Cardiovascular Laboratory, Nanjing First Hospital, Nanjing Medical University, Nanjing, Jiangsu 210006, China;
[3]Division of Cardiology, Shanghai General Hospital, School of Medicine, Shanghai Jiao Tong University, Shanghai 200080, China;
[4]Division of Pulmonary Surgery, Wuxi People's Hospital, Nanjing Medical University, Wuxi, Jiangsu 300247, China;
[5]Institute of Vascular Medicine, The Chinese University of Hong Kong, Hongkong 999077, China;
[6]Health Science Center, East China Normal University, Shanghai 200241, China;
[7]School of Pharmacy, Nanjing Medical University, Nanjing, Jiangsu 210004, China;
[8]Division of Cardiology, Nanjing First Hospital, Nanjing Medical University, Nanjing, Jiangsu 210006, China.

Abstract

Background: Pulmonary arterial hypertension (PAH) is characterized by excessive proliferation of small pulmonary arterial vascular smooth muscle cells (PASMCs), endothelial dysfunction, and extracellular matrix remodeling. G protein-coupled receptor kinase 2 (GRK2) plays an important role in the maintenance of vascular tone and blood flow. However, the role of GRK2 in the pathogenesis of PAH is unknown.

Methods: GRK2 levels were detected in lung tissues from healthy people and PAH patients. C57BL/6 mice, vascular smooth muscle cell-specific *Grk2*-knockout mice ($Grk2^{\Delta SM22}$), and littermate controls ($Grk2^{flox/flox}$) were grouped into control and hypoxia mice ($n = 8$). Pulmonary hypertension (PH) was induced by exposure to chronic hypoxia (10%) combined with injection of the SU5416 (cHx/SU). The expression levels of GRK2 and Yes-associated protein (YAP) in pulmonary arteries and PASMCs were detected by Western blotting and immunofluorescence staining. The mRNA expression levels of *Grk2* and Yes-associated protein (*YAP*) in PASMCs were quantified with real-time polymerase chain reaction (RT-PCR). Wound-healing assay, 3-(4,5)-dimethylthiahiazo (-z-y1)-3,5-di-phenytetrazoliumromide (MTT) assay, and 5-Ethynyl-2′-deoxyuridine (EdU) staining were performed to evaluate the proliferation and migration of PASMCs. Meanwhile, the interaction among proteins was detected by immunoprecipitation assays.

Results: The expression levels of GRK2 were upregulated in the pulmonary arteries of patients with PAH and the lungs of PH mice. Moreover, cHx/SU-induced PH was attenuated in $Grk2^{\Delta SM22}$ mice compared with littermate controls. The amelioration of PH in $Grk2^{\Delta SM22}$ mice was accompanied by reduced pulmonary vascular remodeling. *In vitro* study further confirmed that *GRK2* knock-down significantly altered hypoxia-induced PASMCs proliferation and migration, whereas this effect was severely intensified by overexpression of *GRK2*. We also identified that GRK2 promoted YAP expression and nuclear translocation in PASMCs, resulting in excessive PASMCs proliferation and migration. Furthermore, GRK2 is stabilized by inhibiting phosphorylating GRK2 on Tyr86 and subsequently activating ubiquitylation under hypoxic conditions.

Conclusion: Our findings suggest that GRK2 plays a critical role in the pathogenesis of PAH, via regulating YAP expression and nuclear translocation. Therefore, GRK2 serves as a novel therapeutic target for PAH treatment.

Keywords: Pulmonary arterial hypertension; GRK2; YAP; Pulmonary artery smooth muscle cell; Hypoxia

Introduction

Pulmonary arterial hypertension (PAH) is an intractable disease characterized by progressively increasing pulmonary vascular resistance (PVR) and the development of right heart failure, leading to premature death.[1–3] The pathogenesis of PAH includes sustained vasoconstriction and abnormal progressive fixed vascular remodeling. This is accompanied by endothelial dysfunction and activation of fibroblasts and smooth muscle cells (SMCs). The PAH survival rate has dramatically improved[4] since the

Access this article online

Quick Response Code:

Website: www.cmj.org

DOI: 10.1097/CM9.0000000000002946

Correspondence to: Shaoliang Chen, Division of Cardiology, Nanjing First Hospital, Nanjing Medical University, Nanjing, Jiangsu 210006, China
E-Mail: chmengx@126.com

Chinese Medical Journal 2024;137(7)

Received: 01-11-2022; **Online:** 19-01-2024 **Edited by:** Rongman Jia and Xiuyuan Hao

Food and Drug Administration (FDA) approval of five classes of agents targeting the three main PAH signaling pathways, including endothelin receptor, cyclic adenosine monophosphate, and phosphodiesterase type-5. Emerging data, however, suggest that the long-term benefits of monotherapy or sequential combinations in treating PAH are still uncertain,[2–4] largely because PAH pathobiology is not fully understood.[5,6] Therefore, the identification and characterization of new therapeutic targets is a pressing need.

The G protein-coupled receptor kinases (GRKs) are a seven-member (GRK1–GRK7) family of serine-threonine protein kinases with different tissue distributions, subcellular localizations, and functions.[6,7] G protein-coupled receptor kinase 2 (GRK2) is the best characterized GRK: it is a cytoplasmic protein that translocates to the plasma membrane upon G protein-coupled receptor (GPCR) stimulation. Once at the plasma membrane, GRK2 specifically recognizes and phosphorylates agonist-activated GPCRs, leading to receptor desensitization and non-responsive to cardiovascular drugs.[7] GRK2 expression has been implicated in the development of heart failure, atherosclerosis, Alzheimer's disease, inflammatory disease, and cancer through modulating GPCR-dependent and GPCR-independent pathways.[6–10] Moreover, GRK2 mediates cell-cycle G2/M progression and the migration and differentiation of vascular smooth muscle cells (SMCs), thus participating in the maintenance of vascular tone and blood flow.[9,10] In two recent studies, Sikka *et al*[11] and Barreto Ortiz *et al*[12] reported that GRK2 inhibition enhanced the photorelaxation of the pulmonary artery induced by repeated blue light exposure. Additionally, both Piao *et al*[13] and Rodriguez-Serrano *et al*[14] showed that inhibiting Gβγ–GRK2 interactions improved sensitization of the failing myocardium induced by PAH. Although GRK2 is clearly implicated in a number of processes critical to the vasculature, its role in pulmonary arterial vascular smooth muscle cells (PASMCs) and PAH has not been fully explored.

HIPPO signaling pathway is a master regulator of cell proliferation, differentiation, and apoptosis.[15] Yes-associated protein (YAP) is a major downstream effector of the HIPPO pathway. When phosphorylated, YAP is stabilized in the cytoplasm by binding to 14-3-3 protein. When dephosphorylated, activated YAP translocates into the nucleus to bind the TEA domain (TEAD) transcription factor, resulting in extracellular matrix (ECM) composition, and the transcription of growth-promoting genes, therefore contributing to cells proliferation and migration,[15–18] and participating in the PAH development.[17–19] Furthermore, YAP and transcriptional coactivator with PDZ-binding motif (TAZ) promote the proliferation and migration of PASMCs and small pulmonary arterial remodeling in idiopathic PAH.[17–19] Importantly, the HIPPO pathway can be regulated by GPCR signaling. Activation of Gs-coupled receptors increased LATS1/2 kinase activity, thus resulting in the inhibition of YAP function.[16] G protein-coupled bile acid receptor activation can control YAP activity and regulate distinct functions of cell growth and apoptosis.[20] Therefore, we hypothesized that GRK2, a regulator of GPCR, modulated the YAP signaling and contributed to PAH in mice and humans.

Methods

Human hemodynamic measurements and lung tissue processing

This study was approved by the Institutional Review Board of Nanjing First Hospital, Nanjing Medical University (No. KY20220425-09), which was in accordance with the *Declaration of Helsinki* regarding investigations in humans, and written consent was obtained from all patients.

Human pulmonary hemodynamics and pulmonary arterial pressure were measured using a 7.5F flow-directed Swan-Ganz catheter (774P75, Edwards Lifesciences LLC, Irvine, CA, US), according to a standard protocol. The pulmonary arteries were extracted from two non-transplantable normal donor lungs, in addition to the adjacent normal lung tissue in a lung cancer patient, and the lungs of six patients undergoing lung transplantation at the Lung Transplant Group, Affiliated Wuxi People's Hospital of Nanjing Medical University. Of these six patients who underwent lung transplantation, three patients had mild pulmonary hypertension (PH; average value of systolic pulmonary arterial pressure [sPAP] was 46 mmHg) secondary to severe lung disease (one with chronic obstructive pulmonary disease and two with idiopathic pulmonary fibrosis), and another three subjects were diagnosed with non-familial PAH (average value of sPAP was 93 mmHg). Human PASMCs were isolated from the lung tissues of normal donors and patients with PH.

Experimental hypoxic PAH modeling and grouping

All experiments involving animals were approved by the Institutional Animal Care and Use Committee of Nanjing First Hospital, Nanjing Medical University (No. DWSY-23110414).

A single intraperitoneal injection of SU5416 (a vascular endothelial growth factor (VEGF) receptor inhibitor, 20 mg/kg, weekly, subcutaneous injection; Sigma–Aldrich, St. Louis, MO, USA) on day 1 was followed by exposure to normobaric hypoxia (5.5 L/min flow of hypoxic air with 10% O_2 and 90% N_2) from day 2 to day 29 to establish hypoxic PH model. Chambers were opened twice weekly for cleaning and replacement of food and water. The oxygen concentration was monitored continuously in the model-making period. Mice exposed to normoxic conditions (21% oxygen) were kept in the same room on the same 12-hour light/12-hour dark cycle as mice exposed to hypoxia. Male C57BL/6J mice (8 weeks old, 20–25 g) (n = 6–8 for each group) were obtained from GemPharmatech company in Nanjing, China. Mice were randomly assigned to the control group or the experimental group, allowing researchers to perform blinded procedures and histological analyses.

SMC-specific Grk2 over-expression or Grk2 knock-down mice

SMC-specific Grk2 over-expression mice were treated with the adeno-associated virus (AAV)-SM22 (smooth muscle protein 2) α-3Flag-SV40 PolyA contained a transcript of the mouse *Grk2* gene (NCBI Reference Sequence: NM_130863.2, produced by Genechem Co. Ltd., Shanghai, China) by tail vein injection.

Grk2 knock-down mice were created by tail vein injection with an adeno-associated virus carrying adeno-associated virus 9 (AAV9)-shGRK2 (shRNA-*GRK*) (5′-GCAAGUGUCUCCUGCUUAATT-3′, 5′-UUAAGCAGGAGACACUUGCT-3′, AAV9-shRNA; 1×10^9 PFU (plaque forming unit) per mice, also produced by Genechem Co. Ltd. Two weeks later, the mice in this study were randomly exposed to hypoxia plus SU5416 (PH model) or 21% oxygen (control group).

SMC-specific Grk2 knock-out mice

$Grk2^{flox/flox}$ ($Grk2^{f/f}$) mice (Stock No. 012458, GRK2tm1Gwd/J; The Jackson Laboratory, Bar Harbor, ME, USA) were crossed with SM22α-CRE (cyclization recombinase) mice (provided by Genetic Animal Center, Nanjing University, Nanjing, China). SM22α-CRE+$Grk2^{f/-}$ mice were crossed with $Grk2^{f/f}$ mice to generate mice with SMC-specific deletion of *Grk2* ($Grk2^{\Delta SM22}$). All mice used in this study were bred on a congenic 129/C57BL6 background. The Grk2 wild type (WT) and Grk2 floxed alleles were verified by polymerase chain reaction (PCR), using the following primers: 5′-TGAGGCTCAGGGATACCTGTCAT-3′ and 5′-CAGGCATTCCTGCTGGACTAG-3′. Mice harboring the SMC-specific Grk2 allele deletion were also genotyped for CRE by PCR, using the following primers: 5′-TGCCACGACCAAGTGACAGCAATG-3′; 5′-ACCAGAGACGGAAATCCATCGCTC-3′. $Grk2^{f/f}$ and SMC-specific *Grk2* knockout mice were randomly divided into three groups: the $Grk2^{f/f}$ group, the $Grk2^{f/f}$ PH group (PH model), and the $Grk2^{\Delta SM22}$ PH group (SMC-specific *Grk2* knockout PH model).

Classification of muscularization of small pulmonary artery

The degree of muscularization of small pulmonary arteries (<150 μm) was defined in accordance with the methods of a previous study.[21]

Hemodynamic measurements, pulmonary angiography, and right ventricle (RV) weight calculation

Right ventricular systolic pressure (RVSP) was measured by right heart catheterization, as previously described.[19] Mice were anesthetized with continuous isoflurane (1%) inhalation. To expose the heart, a small left oblique thoracotomy was performed at the left third to fourth intercostal space. Probes were then inserted into the right ventricle and the waveform was recorded. Pulmonary angiography using polysilicon was performed, as previously described.[19] All animals were sacrificed, and the lung and heart tissues were harvested after hemodynamic measurements were obtained. The right ventricle was then dissected from the left ventricle and septum, and the ventricles were weighed separately. The right ventricle hypertrophy index (RVHI) was defined as the ratio of the weight of the RV to the weight of the left ventricle with the septum.

Histological and immunohistochemical analyses

Animals were sacrificed and the lungs were removed, perfused with ice-cold saline to remove the blood and fixed in 4% paraformaldehyde solution. The lungs were cut into 5-μm-thick sections for hematoxylin and eosin (H&E) staining, according to the manufacturer's protocols. Images were captured under a light microscope (original magnification, 200×; Nikon, Tokyo, Japan).

Isolation and culture of human PASMCs

The isolation, culture, and identification of human PASMCs from 500 μm to 1500 μm-diameter arterioles from patients with or without PAH were performed, as previously described.[22] Human PASMCs were obtained from ScienCell Research Laboratory (Carlsbad, CA, USA) and cultured in smooth muscle cell growth medium (SMGM) containing 5% fetal bovine serum (FBS), 100 U/mL penicillin, and 100 μg/mL streptomycin in a humidified incubator at 37°C with 5% CO_2. During the experiment, the cells were cultured in serum-free medium for 12 h, the proteasome inhibitor MG132 (0.2 μmol/L, Selleck, Houston, TX, USA), or the protein synthesis inhibitor cycloheximide (15 μmol/L, Selleck), followed by exposure to hypoxia (3% oxygen).

PASMCs proliferation and migration assays

PASMCs migration was assessed by wound healing assay and Boyden chamber migration assay, as previously described.[21]

Western blotting

Cell lysates of small pulmonary arteries from patients or donors, lung tissue samples from mice, or PASMCs were prepared as previously described.[21] Protein samples were extracted from nuclear and cytoplasmic fractions were performed using a nuclear and cytoplasmic extraction kit (Thermo Fisher Scientific, Waltham, MA, USA), according to the manufacturer's instructions. The antibodies used include GAPDH, β-actin, phospho-AKT (Ser473), AKT, YAP, H3, E3 ubiquitin-protein ligase Mdm2 (MDM2) (all used at 1:1000; Cell Signaling Technology Inc., Beverly, MA, USA), phospho-GRK2 (Tyr86, Try13, Try92), or GRK2 (1:200; Santa Cruz, CA, USA). The immunoreactive protein bands were scanned by chemiluminescence system (Syngene, Cambridge, UK). Densitometric analysis of immunoblots was performed using ImageJ software (National Institutes of Health, Bethesda, MD, USA).

Real-time PCR (RT-PCR)

Total RNA was extracted from tissues or cells using Trizol reagent (Vazyme Biotech, Nanjing, China) according to the manufacturer's instructions. RNA was

reverse-transcribed into cDNA using HiScript® III RT SuperMix for qPCR (+gDNA wiper) (Vazyme Biotech, Nanjing, China) and quantitative RT–PCR was conducted using Taq Pro Universal SYBR qPCR Master Mix (Vazyme Biotech, Nanjing, China) and ABI 7500 Fast Real-Time PCR system (Applied Biosystem, Calsbad, CA, USA). Primers were designed according to known mouse gene sequences listed in Supplementary Table 1, http://links.lww.com/CM9/B818.

Immunoprecipitation (IP)

For IP, cells were lysed in buffer containing 25 mmol/L N-2-hydroxyethylpiperazine-N-ethane-sulphonicacid (HEPES), 1 mmol/L ethylene diamine tetraacetic acid (EDTA), 125 mmol/L NaCl, 0.5 mmol/L NaF, 0.25% Nonidet P-40, 5% glycerol (pH 6.8), 10 μg/mL leupeptin, 20 μg/mL aprotinin, and 1 mmol/L phenylmethylsulfonyl fluoride. The lysates were centrifuged at 15,000 × *g* for 10 min, and the supernatants were collected. Antibodies specific for GRK2, MDM2 (Cell Signaling Technology) were added to the supernatants and vibrated at 4°C overnight. The resulting immune complexes were isolated with protein A/G-agarose beads (2 h, vibrating, at room temperature). The bound proteins were eluted off the beads and were analyzed by Western blotting with anti-GRK2 antibodies.

Small interfering RNA (siRNA) and plasmids transfection

GRK2-siRNA (5′-GGGAUCUUCGACUCAUATT-3′; 5′-UAUGAGUCGAAGAUCUCCCTT-3′) and scrambled control sequences were obtained from GenePharma (Shanghai, China). Wild-type GRK2 (named WT-GRK2), GRK2 (Tyr86 site mutant to Asp, Tyr86-Asp), and HA (human influenza hemagglutinin)-Ub plasmids were bought from Addgene, Watertown, MA, USA. They were transfected into PASMCs using Lipofectamine 3000 (Invitrogen, Carlsbad, CA, USA) according to the manufacturer's protocol. After transfection for 6 h, the medium was replaced with SMGM supplemented with 5% serum.

Adenoviral overexpression of GRK2

PASMCs were seeded at 5×10^5 cells per 35-mm-diameter well and after 12 h, cell growth was arrested by washing three times with PBS before adding FBS-free OptiMEM. The cells were cultured at 37°C in 5% CO_2 with adenovirus expressing either human GRK2 cDNA driven by the cytomegalovirus early promoter (Ad-GRK2) or an empty vector (Ad-NC).

Immunofluorescence staining

Frozen lung tissue sections and cells were blocked at non-specific sites with 5% albumin from bovine serum (BSA) for 1 h, the sections and cells were incubated with primary antibodies against GRK2 (1:20) or α-SMA (smooth muscle actin) (1:100) overnight at 4°C. After labeling with Alexa 488/555 secondary antibodies (1:200, green, Cell Signaling Technology), sections or cells were counterstained with 4′,6-diamidino-2-phenylindole (DAPI). Fluorescence images were acquired using a confocal laser scanning microscope Zeiss LSM 880 (Oberkochen, Germany).

Statistical analysis

Data are expressed as the mean ± standard error of the mean (SEM). Statistical analyses of differences between groups were performed using Student's *t*-test. One-way analysis of variance (ANOVA) with Bonferroni correction was used for multiple group comparisons. Equivalence of variance between groups was confirmed using an *F*-test for comparisons between two groups and a Brown–Forsythe test in conjunction with ANOVA, when applicable. Normal distribution was assumed for all statistical analyses and confirmed when group sizes allowed for testing of normality. The difference in muscularization was analyzed using chi-squared or exact test. All statistical tests used two-sided tests of significance. GraphPad Prism 8 (www.dotmatics.com) was applied, and $P < 0.05$ indicated statistically significant differences.

Results

GRK2 was associated with PAH and PAH disease severity

We first aimed to establish an involvement of GRK2 in PAH. To this end, we compared the protein levels in pulmonary artery (PA) isolated from three normal donor lungs and six recipient lungs. Of these six patients who underwent lung transplantation, three patients had mild pulmonary hypertension (PH) secondary to severe lung disease (one with chronic obstructive pulmonary disease and two with idiopathic pulmonary fibrosis) and another three subjects had severe non-familial PAH [Figure 1A]. We found that GRK2 protein levels in PA from three severe PAH patients were 5.2-fold higher than those from donor lungs and 2.5-fold higher than those from three patients with mild pulmonary hypertension [Figure 1A]. For further validation, GRK2 expression and distribution were determined via immunofluorescence. Immunofluorescence staining of PA of PAH patients demonstrated that GRK2 was highly expressed in the thickened medial layer [Figure 1B]. We then compared GRK2 protein expression in lung tissues taken from mice with hypoxia-induced PAH (cHx/SU) and control mice. Similar to the human data, higher GRK2 levels were detected in lung tissues from PH mice than those from normoxia control mice [Figure 1C], mainly expressed in the thickened medial layer [Figure 1D].

To confirm this finding in an *in vitro* system, we cultured human PASMCs under hypoxic conditions (3% oxygen) for various lengths of time and found a time-dependent elevation in GRK2 protein expression [Figure 1E]. To identify if the difference in GRK2 protein expression exists between PAH and non-PAH PASMCs, we isolated and sub-cultured PASMCs from the small PA of three PAH patients and three controls [Figure 1F]. We observed a higher level of GRK2 protein in PASMCs from PAH patients than those from controls.

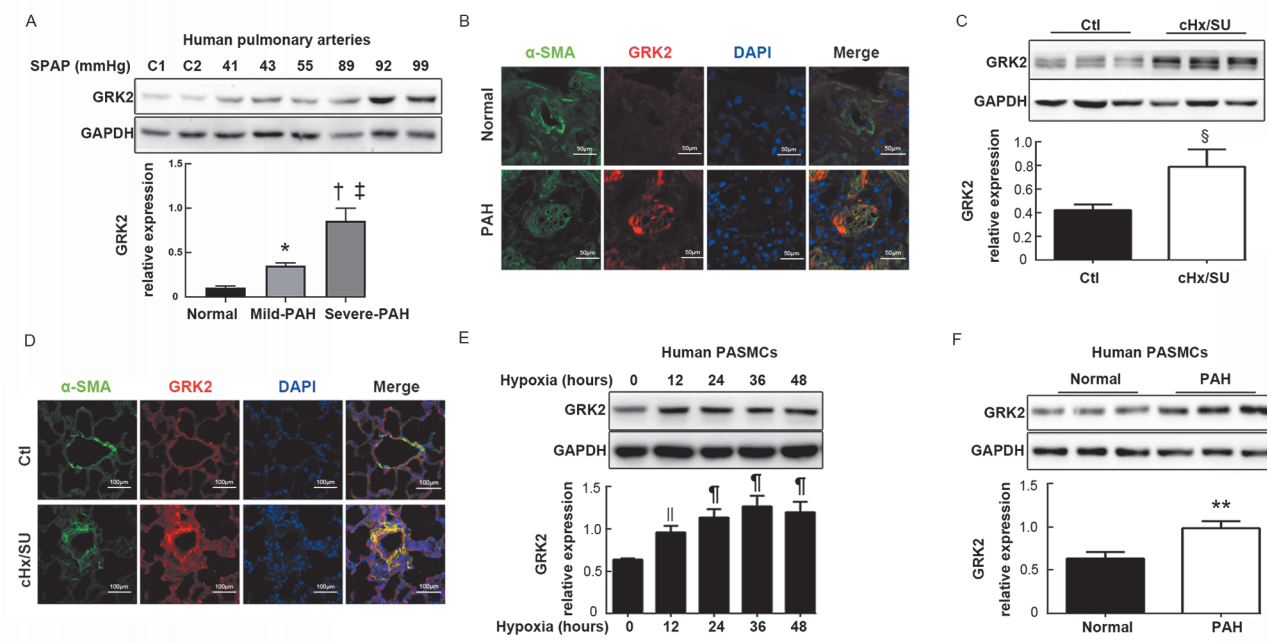

Figure 1: GRK2 is associated with PAH and PAH disease severity. (A) Western blotting analysis of GRK2 expression in pulmonary arterial vessels of healthy donors and patients with different systolic pulmonary arterial pressures ($n = 3$). (B) GRK2 (red) and α-SMA (green) immunofluorescence staining in small pulmonary arteries from humans with or without PAH. Nuclei are counterstained with DAPI (blue) ($n = 8$). Scale bar, 50 μm. (C) GRK2 expression in lung tissues of mice with hypoxia (cHx)/SU5416 (Su)-induced PAH compared to that in control mouse lungs ($n = 8$). (D) GRK2 (red) and α-SMA (green) immunofluorescence staining in small pulmonary arteries from mice with or without cHx/SU-induced PAH ($n = 8$). Scale bar, 100 μm. (E) The level of GRK2 protein in human PASMCs stimulated with hypoxia at various time points ($n = 3$). (F) GRK2 expression in sub-cultured PASMCs derived from the lungs of three normal controls (normal) and three patients with PAH (PAH = 78, 89, and 92 mmHg) ($n = 3$). $^{*}P < 0.05$ and $^{\dagger}P < 0.001$ *vs.* normal, $^{\ddagger}P < 0.001$ *vs.* mild-PAH, $^{\S}P < 0.001$ *vs.* Ctl, $^{\|}P < 0.01$ and $^{\P}P < 0.001$ *vs.* Ctl, $^{**}P < 0.01$ *vs.* normal. The data represent the means ± SEM. α-SMA: α-smooth muscle actin; cHx/SU: Hypoxia + SU416; Ctl: Control; DAPI: 4′,6-diamidino-2-phenylindole; GAPDH: Glyceraldehyde 3-phosphate dehydrogenase; GRK2: G protein-coupled receptor kinase 2; PAH: Pulmonary arterial hypertension; PASMCs: Pulmonary arterial smooth muscle cells; SEM: Standard error of the mean; SPAP: Systolic pulmonary artery pressure.

GRK2 plays a critical role in the development of PH induced by hypoxia

Our data confirmed increased GRK2 protein level in PA of PAH. However, the consequences of GRK2 down-regulation on PASMCs proliferation/migration or PAH progression are unknown. We thus studied the effect of GRK2 down-regulation on PAH development in mice via tail vein injection of adeno-associated virus 9 (AAV9) carrying a GRK2 short hairpin RNA (AAV-GRK2 shRNA). Analyses by immunofluorescence staining and Western blotting showed efficient downregulation of GRK2 in lungs of AAV-GRK2 shRNA-treated mice compared with controls [Supplementary Figure 1, http://links.lww.com/CM9/B818]. We observed GRK2 down-regulation in normoxic mice did not change RVSP [Figure 2A,B] and right ventricle hypertrophy index (RVHI) [Figure 2C]. Hypoxia-induced increases of RVSP and RVHI were significantly reversed by GRK2 down-regulation [Figure 2A–C].

To assess the anatomical change of the pulmonary artery caused by GRK2 down-expression under hypoxia, we then performed mouse pulmonary angiography and found that compared to hypoxic mice, hypoxic mice treated with GRK2 shRNA exhibited diffuse vascular blush consistent with a patent distal pulmonary vascular tree [Figure 2D]. Distal small PA normally has no or very less SMCs and will develop severe PASMCs proliferation (i.e., muscularization) during PAH development.[4–6] Therefore, we measured the improvement of muscularization by GRK2 down-regulation in mice. Figure 2E,F illustrate that GRK2 down-regulation revealed a lower degree of both partial (defined as H&E staining 25–75%) and full (defined as H&E staining >75%) muscularization in mice under hypoxia. The improvements in muscularization by GRK2 down-regulation resulted in a significant reduction in wall thickness [Figure 2G]. The messenger RNA (mRNA) levels of molecules involved in vascular remodeling, such as SM22α, smooth muscle myosin heavy chain (SMMHC), monocyte chemoattractant protein-1 (MCP-1), matrix metalloproteinase 2 (MMP2), matrix metalloproteinase 99 (MMP), connective tissue growth factor (CTGF), Collagen I, Collagen III, and Vimentin were significantly increased in the pulmonary arteries of hypoxic mice and down-regulation of GRK2 reversed these changes [Figure 2H]. Furthermore, paroxetine is a potent GRK2 inhibitor with higher selectivity for GRK2. Compared to hypoxic mice, using paroxetine significantly prevents the development of PAH as determined by the reduction of RVSP, RVHI muscularization, and wall thickness [Supplementary Figure 2, http://links.lww.com/CM9/B818].

We next investigated the consequences of GRK2 up-regulation in mice with smooth muscle cell-targeted GRK2 overexpression (SMC-GRK2). The SMC-specific transgene expression of GRK2 was achieved by AAV9. Immunofluorescence staining showed PASMCs-specific upregulation of GRK2 in the lungs of SMC-GRK2 mice compared with controls [Supplementary Figure 3, http://links.lww.com/CM9/B818]. Under hypoxic conditions, GRK2 over-expression displayed a much more severe

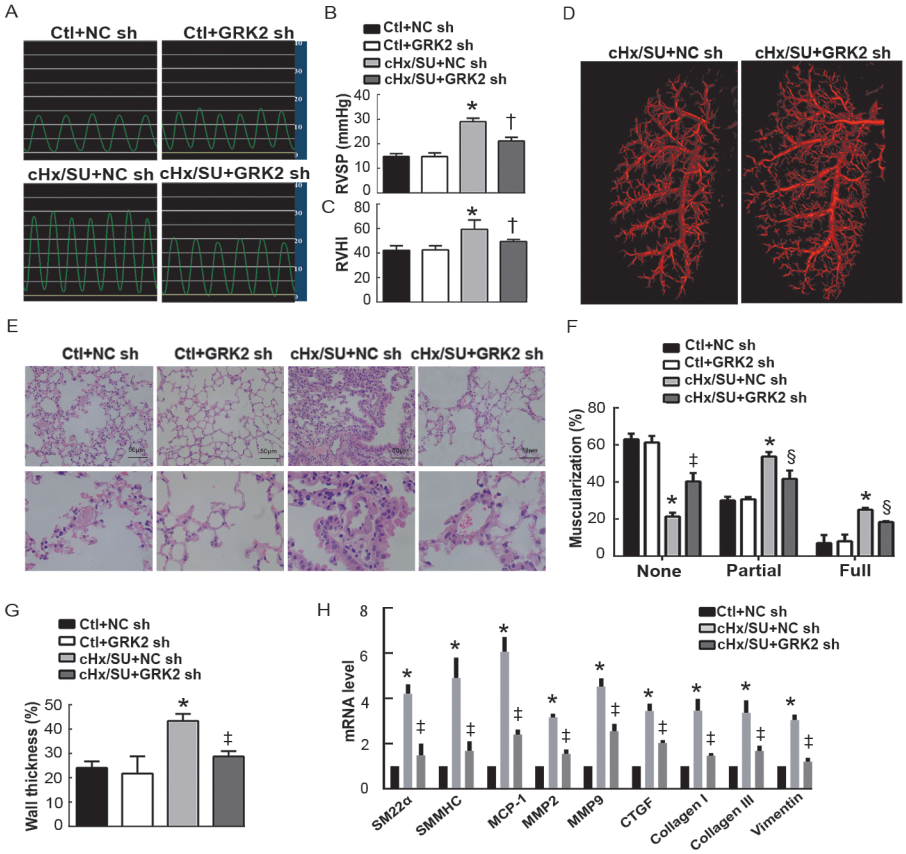

Figure 2: GRK2 down-regulation in PASMCs ameliorates PAH features *in vivo*. (A) Representative images of RVSP waves in control + NC shRNA (Ctl + NC sh) mice, Ctl + GRK2 shRNA (Ctl + GRK2 sh) mice, cHx/SU + NC shRNA (cHx/SU + NC sh) mice, and cHx/SU+ GRK2 shRNA (cHx/SU + GRK2 sh) mice ($n = 8$). (B) Assessment of RVSP in each group ($n = 8$). (C) RVHI calculated by the right ventricle to left ventricle + septum (RV/LV + S) weight ratios in each group ($n = 8$). (D) Representative images of pulmonary angiograms of cHx/SU + NC mice and cHx/SU + GRK2 shRNA mice ($n = 6$). (E) H&E-stained sections of small pulmonary arteries from each group ($n = 8$). Scale bar, 50 μm. (F) None, partial, and full muscularization of pulmonary arteries are shown as percentages ($n = 8$). (G) Assessment of the pulmonary arterial wall thickness as a percentage of the luminal diameter ($n = 8$). (H) RT-PCR assessment of the mRNA level of SM22α, SMMHC, MCP-1, MMP2, MMP9, CTGF, Collagen I, Collagen III, and Vimentin in the lungs of each group ($n = 8$). $^{*}P < 0.001$ *vs.* Ctl + NC sh. $^{§}P < 0.05$, $^{†}P < 0.01$ and $^{‡}P < 0.001$ *vs.* cHx/SU + NC sh. The data represent the means ± SEM. AAV9: Adeno-associated virus 9; cHx/SU: Hypoxia/SU5416; Ctl: Control; CTGF: Connective tissue growth factor; GRK2: G protein-coupled receptor kinase 2; H&E: Hematoxylin and eosin; MCP-1: Monocyte chemoattractant protein 1; MMP2: Matrix metallopeptidase 2; MMP9: Matrix metallopeptidase 9; mRNA: Messenger Ribonucleic acid; NC: Null control; PAH: Pulmonary arterial hypertension; PASMCs: Pulmonary arterial smooth muscle cells; RT-PCR: Real-time Polymerase Chain Reaction; RVHI: Right ventricle hypertrophy index; RVSP: Right ventricular systolic pressure; SEM: Standard error of the mean; SM22α: Smooth muscle protein 22-α; SMMHC: Smooth muscle myosin heavy chain.

PH phenotype than control mice as determined by RVSP [Figure 3A,B] and RVHI [Figure 3C]. To assess the anatomical change of the pulmonary artery caused by hypoxia, we performed mouse pulmonary angiography, and observed small vessel occlusion in hypoxic mice, with an increase in the severity of occlusion in SMC-specific GRK2 over-expression mice under hypoxia [Figure 3D]. Next, we also measured muscularization in the small PA. Compared to normoxic mice, littermates exposed to hypoxia exhibited severe muscularization that was either partial or full [Figure 3E,F]. Compared to the hypoxic condition alone, SMC-specific GRK2 over-expression under hypoxia exposure had no effect on the percentage of partial muscularization, but significantly further increased full muscularization [Figure 3E,F], which is consistent with the more profound thickening of the vessel wall [Figure 3G]. The mRNA levels of SM22α, SMMHC, MCP-1, MMP2, MMP9, CTGF, Collagen I, Collagen III, and Vimentin also increased significantly when GRK2 was over-expressed [Figure 3H]. Collectively, these data showed the improvements in small pulmonary arterial remodeling and hypoxia-induced PAH development by GRK2 down-regulation. Furthermore, GRK2 over-expression severely exaggerated hypoxia-induced PAH development.

SMC-specific Grk2 knock-out mice are resistant to PAH development

Our data thus described a protective effect of GRK2 down-regulation against hypoxia-induced PAH. We therefore asked whether SMC-specific GRK2 deletion also affects hypoxia-induced PAH *in vivo*. To do so, we used mice with a homozygous *Grk2* deletion specifically in SMCs ($Grk2^{\Delta SM22}$) [Figure 4A] confirmed by genotypic identification using PCR [Figure 4B] and immunofluorescence staining of lung sections [Supplementary Figure 4, http://links.lww.com/CM9/B818]. Compared to $Grk2^{f/f}$ mice maintained under normoxia that did not develop PAH, $Grk2^{f/f}$ mice exposed to hypoxia for 4 weeks developed

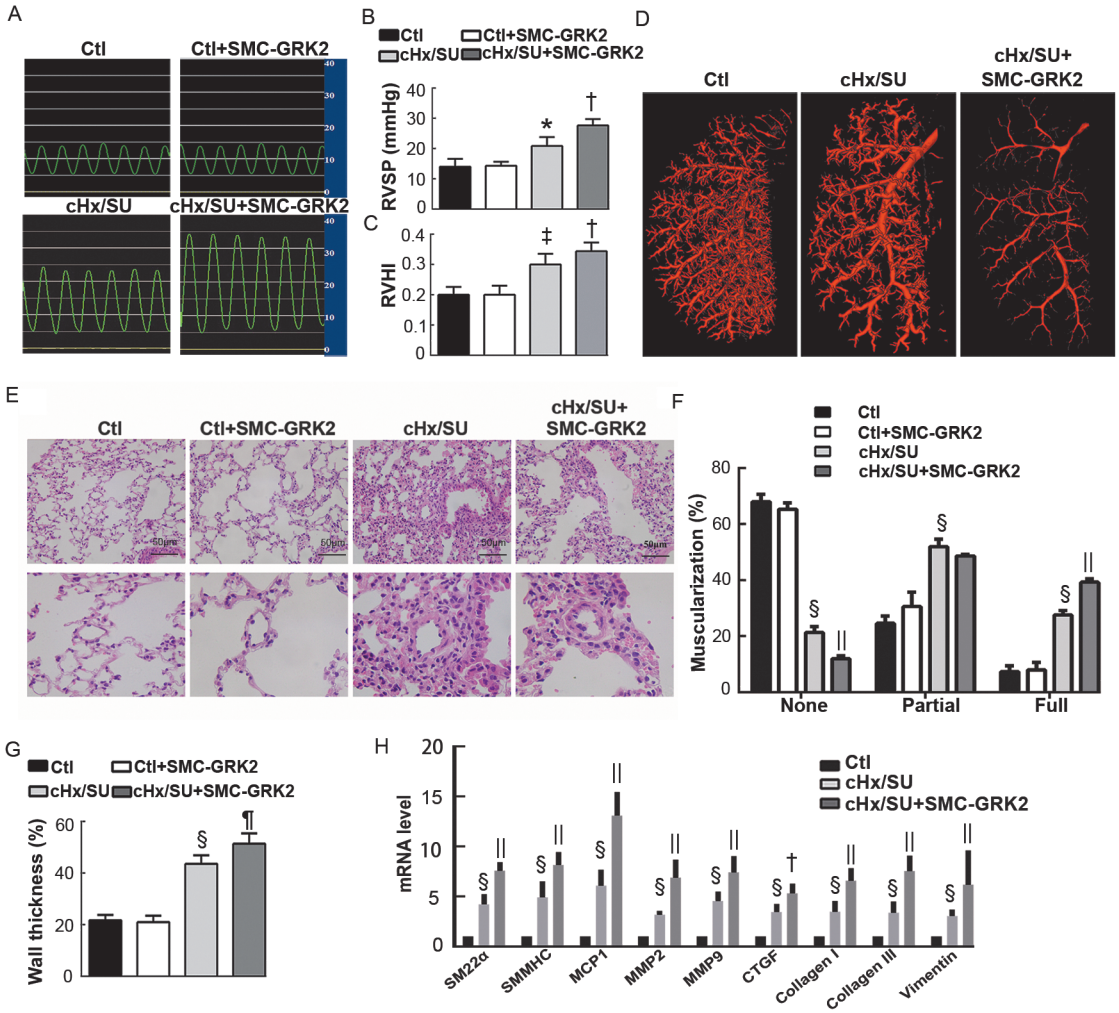

Figure 3: GRK2 up-regulation in PASMCs exacerbates PAH *in vivo*. (A) Representative images of RVSP waves in Ctl mice, AAV9-mediated SMC-specific GRK2 over-expression (Ctl + SMC-GRK2) mice, cHx/SU mice, and cHx/SU + SMC-GRK2 mice ($n = 8$). (B) Assessment of RVSP in each group ($n = 8$). (C) RVHI calculated in each group ($n = 8$). (D) Representative pulmonary angiograms of Ctl, cHx/SU, and cHx/SU+SMC-GRK2 groups ($n = 5$). (E) Representative H&E-stained sections of small pulmonary arteries from the lungs of four groups ($n = 8$). Scale bar, 50 μm. (F) None, partial, and full muscularization of pulmonary arteries are shown as percentages ($n = 8$). (G) Pulmonary arterial wall thickness as a percentage of the luminal diameter ($n = 8$). (H) mRNA level of SM22α, SMMHC, MCP-1, MMP2, MMP9, CTGF, Collagen I, Collagen III, and Vimentin in the lungs of each group ($n = 8$). $^{*}P < 0.05$, $^{‡}P < 0.01$ and $^{§}P < 0.001$ *vs.* Ctl. $^{†}P < 0.05$, $^{¶}P < 0.01$, and $^{‖}P < 0.001$ *vs.* cHx/SU. The data represent the means ± SEM. AAV9: Adeno-associated virus 9; Ctl: Control; cHx/SU: Hypoxia/SU5416; CTGF: Connective tissue growth factor; GRK2: G protein-coupled receptor kinase 2; H&E: Hematoxylin and eosin; MCP-1: Monocyte chemoattractant protein-1; MMP2: Matrix metallopeptidase 2; MMP9: Matrix metallopeptidase 9; mRNA: Messenger Ribonucleic acid; PAH: Pulmonary arterial hypertension; PASMCs: Pulmonary arterial smooth muscle cells; RVHI: Right ventricle hypertrophy index; RVSP: Right ventricular systolic pressure; SEM: Standard error of the mean; SM22α: Smooth muscle protein 22-α; SMC: Smooth muscle cell; SMMHC: Smooth muscle myosin heavy chain.

PAH, as evidenced by an increase in RVSP [Figure 4C,D] and RVHI [Figure 4E]. Pulmonary arterial angiography showed severe occlusion of distal small pulmonary arteries in *Grk2*$^{f/f}$ mice after 4 weeks of exposure to hypoxia [Figure 4F], in consistent with increased muscularization [Figure 4G,H] and vessel wall thickness [Figure 4I]. By contrast, *Grk2*$^{\Delta SM22}$ mice exposed to 4 weeks of hypoxia developed less severe PAH, as evidenced by significant decreases in RVSP [Figure 4C,D] and RVHI [Figure 4E] compared to *Grk2*$^{f/f}$ mice. Angiography confirmed the improved blood flushing and decreased distal small vessel occlusion in *Grk2*$^{\Delta SM22}$ mice after 4 weeks of exposure to hypoxia [Figure 4F]. Furthermore, *Grk2*$^{\Delta SM22}$ mice had almost normal-appearing vessel lumens [Figure 4G] without excessive vessel wall thickening [Figure 4H,I]. Full muscularization in small vessels was significantly reversed in *Grk2*$^{\Delta SM22}$ mice compared to that in *Grk2*$^{f/f}$ mice [Figure 4H]. The mRNA levels of SM22α, SMMHC, MCP-1, MMP2, MMP9, CTGF, Collagen I, Collagen III, and Vimentin were significantly increased in the pulmonary arteries of PAH mice, and GRK2 deficiency in SMCs reversed these changes [Figure 4J]. Taken together, these data support that SMC-specific *Grk2* knock-out prevented PAH development.

GRK2 promotes hypoxia-induced PASMCs proliferation and migration

The proliferation and migration of PASMCs are important factors for vascular-wall remodeling in PAH development. To provide the direct evidence about the change of PASMCs migration and proliferation, wound-healing assay, 3-(4,5)-dimethylthiahiazo (-z-y1)-3,5-di-phenytetrazoliumromide (MTT) assay, and 5-Ethynyl-2′-deoxyuridine (EdU)

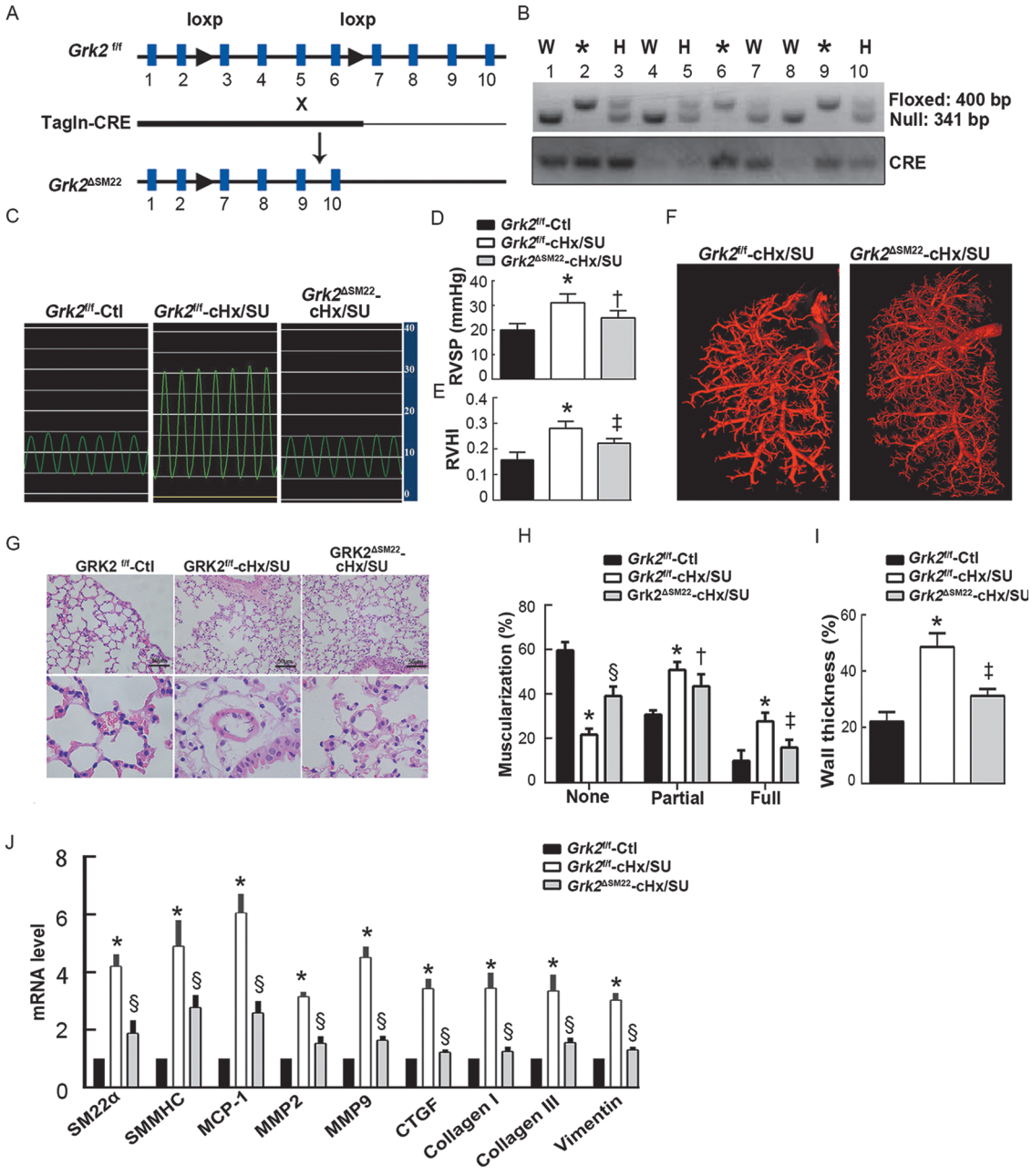

Figure 4: Specific SMC-*Grk2*$^{-/-}$ mice are resistant to PAH development. (A) Schematic of the transgenic mice used to breed SMC-specific *Grk2* knockout (*Grk2*$^{\Delta SM22}$) mice. (B) Genotypic identification of *Grk2*$^{\Delta SM22}$ mice. (C) Representative images of RVSP waves in *Grk2*$^{f/f}$-Ctl mice, *Grk2*$^{f/f}$-cHx/SU mice, and *Grk2*$^{\Delta SM22}$-cHx/SU mice ($n = 10$). (D) Assessment of RVSP in each group ($n = 10$). (E) RVHI calculated in each group ($n = 10$). (F) Representative pulmonary angiograms of *Grk2*$^{f/f}$-cHx/SU mice and *Grk2*$^{\Delta SM22}$-cHx/SU mice. (G) Representative H&E-stained sections of small pulmonary arteries from the lungs of the four groups ($n = 6$). Scale bar, 50 μm. (H) None, partial, and full muscularization of pulmonary arteries are shown as percentages. (I) Pulmonary arterial wall thickness as a percentage of the luminal diameter ($n = 10$). (J) mRNA level of SM22α, SMMHC, MCP-1, MMP2, MMP9, CTGF, Collagen I, Collagen III, and Vimentin in lungs of each group ($n = 10$). $^{*}P < 0.001$ *vs.* *Grk2*$^{f/f}$-Ctl. $^{\dagger}P < 0.05$, $^{\ddagger}P < 0.01$, and $^{\S}P < 0.001$ *vs.* *Grk2*$^{f/f}$-cHx/SU. The data represent the mean ± SEM. bp: Base pair; cHx/SU: Hypoxia/SU5416; CRE: Cyclization recombination; Ctl: Control; CTGF: Connective tissue growth factor; Grk2: G protein-coupled receptor kinase 2; H&E: Hematoxylin and eosin; MCP-1: Monocyte chemoattractant protein-1; MMP2: Matrix metallopeptidase 2; MMP9: Matrix metallopeptidase 9; mRNA: Messenger Ribonucleic acid; PAH: Pulmonary arterial hypertension; RVHI: Right ventricle hypertrophy index; RVSP: Right ventricular systolic pressure; SEM: Standard error of the mean; SM22α: Smooth muscle protein 22-α; SMC: Smooth muscle cell; SMMHC: Smooth muscle myosin heavy chain.

staining were performed in PASMCs. Compared to hypoxia exposure (3% oxygen), GRK2 down-regulation led to a profound inhibition of PASMCs migration [Figure 5A,B] and proliferation [Figure 5C]. Wound-healing assay, MTT assay, and EdU staining also indicated that the knockdown of GRK2 decreased the migration and proliferation potential of PASMCs from PAH patients under normoxic conditions [Figure 5D–F]. Furthermore, results also demonstrated a further increase of PASMCs migration [Figure 5G,H] and proliferation [Figure 5I] worsened by GRK2 over-expression under hypoxia, compared to hypoxia exposure alone. Collectively, these data showed that GRK2 promoted hypoxia-induced proliferation and migration of PASMCs.

GRK2–YAP signaling is involved in PAH

HIPPO pathway is the master regulator of organ growth by limiting cell migration and proliferation.[15] Downstream molecules of the HIPPO pathway have been implicated in PAH, including YAP and phosphorylated AKT-Ser 473.[19] Moreover, GPCRs and their ligands regulate the HIPPO pathway and its downstream signaling molecules in failing myocardium,[16] but a specific interplay between GRK2 and HIPPO-YAP in PASMCs is unknown. In this regard, we thus studied GRK2 and YAP protein levels in PASMCs isolated from human subjects. Indeed, we noted that GRK2 and YAP protein expression and AKT-Ser473 phosphorylation levels were markedly up-regulated in PASMCs from patients with PAH compared to healthy subjects [Figure 6A]. This finding suggests that GRK2, YAP, and AKT-Ser 473 are implicated in PAH development.

To investigate potential YAP-AKT regulation by GRK2, we then studied the change in mRNA and protein levels of YAP and phosphorylation of AKT-Ser 473 induced by GRK2 expression in human donor PASMCs sub-cultured under normoxic and hypoxic conditions. PASMCs exposed to hypoxia exhibited increased YAP and AKT-Ser 473 protein levels. This elevation in YAP protein and AKT-Ser 473 phosphorylation levels was further enhanced upon GRK2 over-expression [Figure 6B], accompanied by increased YAP nuclear translocation [Figure 6C]. Next, we studied the inhibitory effects of GRK2 down-regulation on YAP protein and AKT-Ser 473 phosphorylation levels and found that PASMCs transfected with GRK2 siRNA demonstrated marked reductions in YAP protein expression and AKT-Ser 473 phosphorylation levels [Figure 6D] and YAP nuclear translocation [Figure 6E] under hypoxia conditions. Next, we studied the AKT-Ser 473 regulation by YAP and found that PASMCs transfected with YAP siRNA resulted in a reduction in AKT-Ser 473 phosphorylation under hypoxic exposure [Figure 6F], suggesting YAP functioning as the upstream of AKT. In Supplementary Figure 5, http://links.lww.com/CM9/B818, we found that GRK2 overexpression significantly increased PASMCs proliferation and migration under hypoxia exposure. *YAP* knocked down by siRNA reversed the increase of PASMCs proliferation and migration induced by GRK2 overexpression. As shown in Supplementary Figure 6, http://links.lww.com/CM9/B818, Western blotting showed that YAP was downregulated in the lung tissues in SMC-specific *Grk2* knockout mice compared to control mice under hypoxia conditions. To investigate mechanism by which GRK2

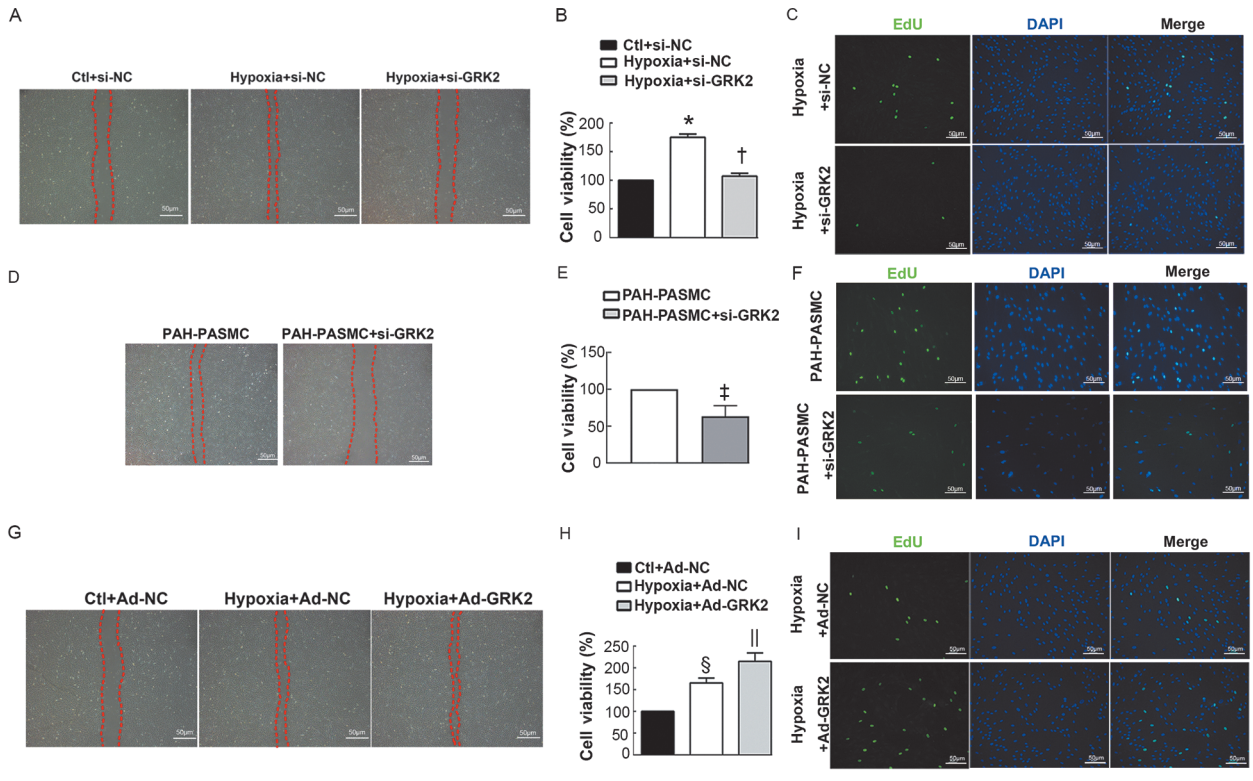

Figure 5: GRK2 promotes hypoxia-induced PASMCs proliferation and migration. (A) Wound healing assay in Ctl + si-NC, hypoxia + si-NC, and hypoxia + si-GRK2 groups. (B, C) The proliferative activity of PASMCs assessed by MTT assay and EdU staining. Representative images of three independent experiments are shown. (D–F) Cell migration and proliferation activity assessed by wound healing assay, MTT assay, and EdU staining in PASMCs from patients with PAH transfected with or without *si-GRK2* ($n = 3$). Representative images of three independent experiments are shown. (G–I) Representative images of the wound healing assay, MTT assay, and EdU staining in Ctl + Ad-NC, hypoxia + Ad-NC, and hypoxia + Ad-GRK2 groups ($n = 3$). Representative images of three independent experiments are shown. $^{*}P < 0.001$ *vs.* Ctl + si-NC, $^{\dagger}P < 0.01$ *vs.* Hypoxia + si-NC, $^{\ddagger}P < 0.001$ *vs.* PAH-PASMC, $^{\S}P < 0.001$ *vs.* Ctl + Ad-NC, $^{\|}P < 0.001$ *vs.* Hypoxia + Ad-NC. The data represent the mean ± SEM. Ad: Adenovirus; Ctl: Control; DAPI: 4′,6-diamidino-2-phenylindole; EdU: 5-Ethynyl-2′-deoxyuridine; GRK2: G protein-coupled receptor kinase 2; MTT: Dimethyl thiazolyl diphenyl tetrazolium salt; NC: Normal control; PAH: Pulmonary arterial hypertension; PASMC: Pulmonary arterial smooth muscle cell; SEM: Standard error of the mean; si: Small interfering.

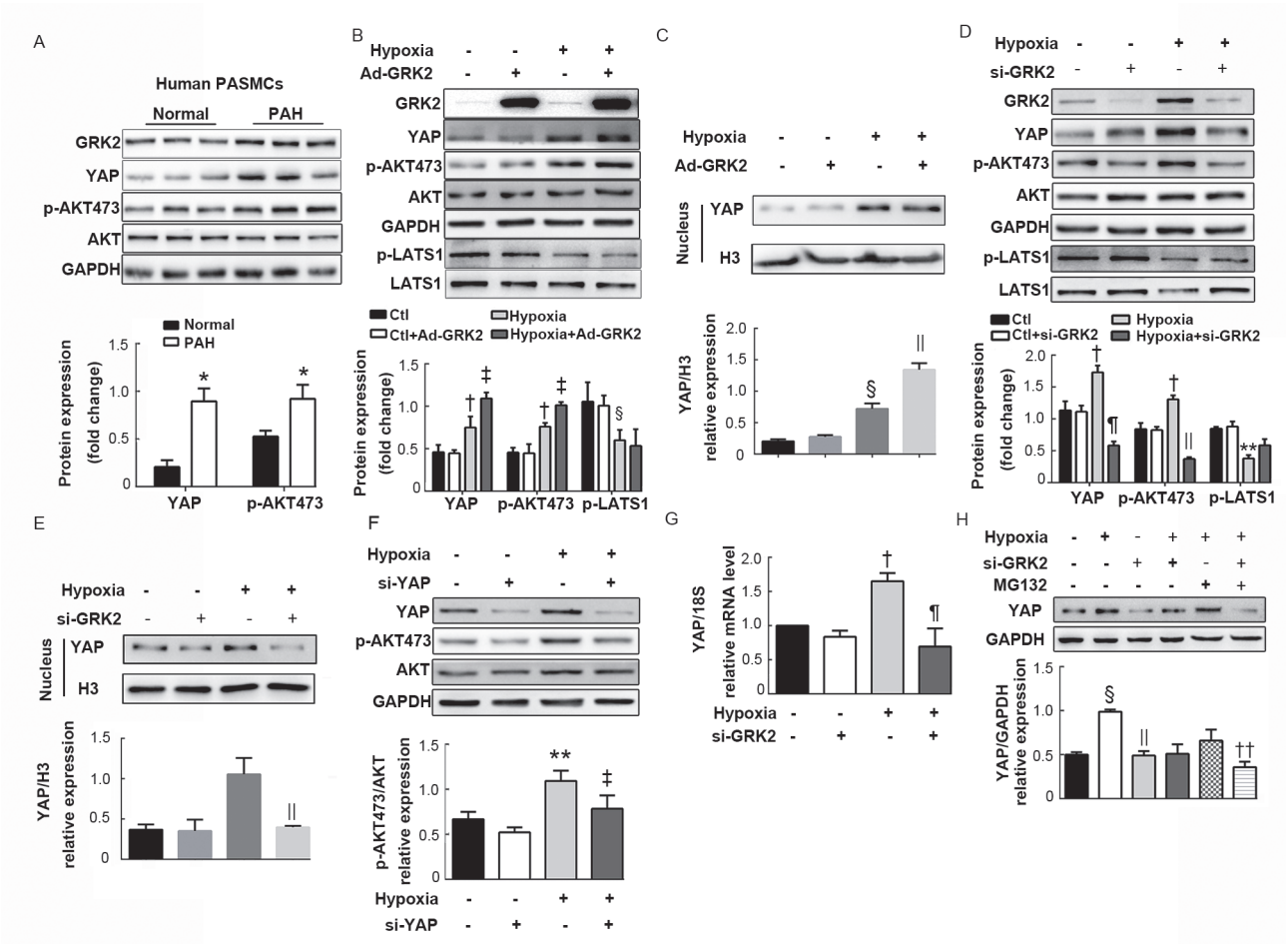

Figure 6: The GRK2-YAP signaling pathway is involved in PAH. (A) Western blotting analysis of GRK2, YAP, and p-AKT473 in pulmonary arteries derived from the lungs of human subjects with or without PAH ($n = 3$). (B) Western blotting analysis of YAP and p-AKT473 in PASMCs transfected with Ad-GRK2 or not and then exposed to hypoxia or normoxia ($n = 3$). (C) Nuclear protein was extracted and the content of YAP was detected by Western blotting ($n = 3$). (D) Western blotting analysis of YAP and p-AKT473 in PASMCs transfected with si-GRK2 or not and exposed normoxia or hypoxia ($n = 3$). (E) Nuclear protein was extracted and the content of YAP was detected by Western blotting. (F) Western blotting analysis of YAP and p-AKT473 in PASMCs transfected with si-YAP or not and then exposed to hypoxia or normoxia ($n = 3$). (G) mRNA level of YAP in PASMCs transfected with si-GRK2 or si-NC and exposed normoxia or hypoxia ($n = 3$). (H) Western blotting analysis of YAP protein under hypoxia or normoxia conditions with or without treatment of MG132 ($n = 3$). $^{*}P < 0.01$ *vs.* Normal, $^{\dagger}P < 0.05$, $^{**}P < 0.01$ and $^{\S}P < 0.001$ *vs.* Ctl, $^{\ddagger}P < 0.05$, $^{\P}P < 0.01$ and $^{\|}P < 0.001$ *vs.* Hypoxia, $^{\dagger\dagger}P < 0.05$ *vs.* Hypoxia + MG132. The data represent the mean ± SEM. Ad: Adenovirus; GAPDH: Glyceraldehyde 3-phosphate dehydrogenase; GRK2: G protein-coupled receptor kinase 2; MG132: Proteasome inhibitor; mRNA: Messenger Ribonucleic acid; PAH: Pulmonary arterial hypertension; PASMC: Pulmonary arterial smooth muscle cell; p-AKT 473: Phosphorylated AKT 473; PASMCs: Pulmonary arterial smooth muscle cells; p-LATS1: Phospho-large tumor suppressor 1; SEM: Standard error of the mean; si: Small interfering; YAP: Yes-associated protein.

regulates YAP, we then examined the mRNA levels of YAP and observed that GRK2 down-regulation suppressed YAP mRNA levels [Figure 6G]. Furthermore, we treated PASMCs with cycloheximide, a protein synthesis inhibitor, under normoxia or hypoxia conditions. As shown in Supplementary Figure 7, http://links.lww.com/CM9/B818, hypoxia exposure showed no effect on the degradation of YAP in the presence of cycloheximide. Next, we treated cells with the proteasome inhibitor MG-132. GRK2 down-regulation significantly decreased the YAP level in PASMCs under hypoxia conditions no matter with or without MG132 treatment [Figure 6H]. These data indicated that *YAP* was up-regulated at a transcriptional level by GRK2 in response to hypoxia. Collectively, we provide evidence that GRK2 might be an upstream mediator of the YAP–AKT signaling pathway by modulating synthesis and nuclear localization of YAP, and it may be by this mechanism that GRK2 contributes to PAH development.

Hypoxia inhibits ubiquitination degradation of GRK2 in PASMCs

Here, our study provides evidence that the protein levels but not the mRNA levels of GRK2 changed in hypoxia compared to normoxia [Figure 7A]. These results suggest that hypoxia-induced up-regulation of GRK2 protein was related to altered protein stability. For this issue, PASMCs were treated with cycloheximide to block protein synthesis and analyzed for GRK2 protein decay over time by Western blotting. We found that GRK2 protein degraded in a time-dependent way under normoxic conditions, while hypoxia treatment resulted in an increase of GRK2 stability in PASMCs [Figure 7B]. GRK2 has been previously described for its degradation by the ubiquitin-proteasome pathway. To address whether GRK2 could be modified by ubiquitin, PASMCs were transiently co-transfected with GRK2 and hemagglutinin (HA)-tagged ubiquitin (HA-Ub) plasmids

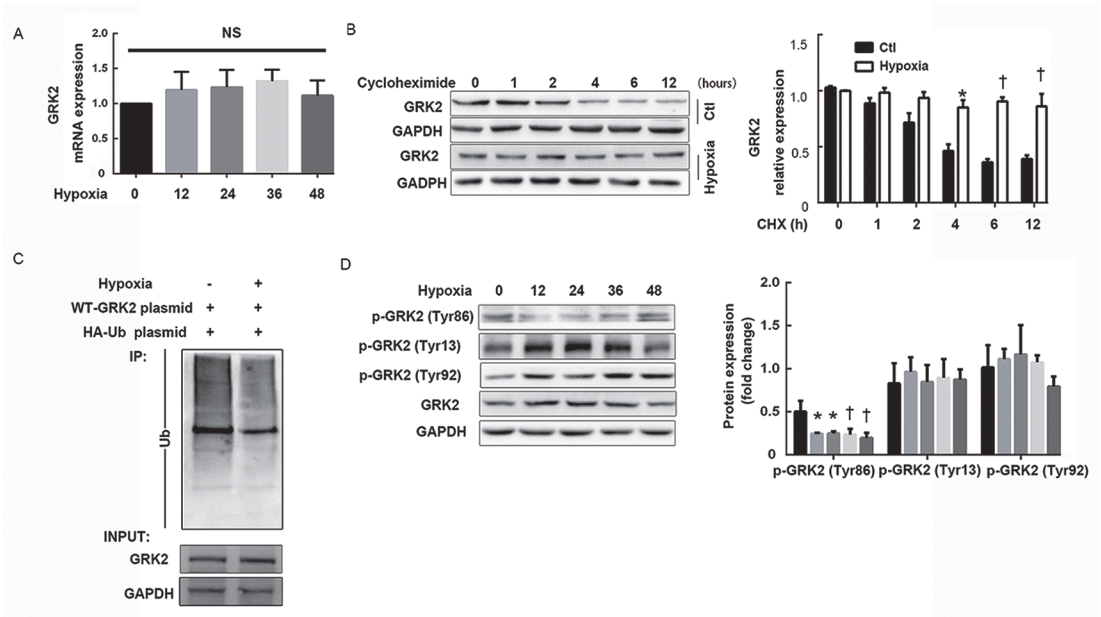

Figure 7: Hypoxia inhibits ubiquitination degradation of GRK2 in PASMCs. (A) mRNA level of GRK2 in PASMC treated with hypoxia for the indicated time points ($n = 3$). (B) Western blotting analysis of GRK2 in PASMCs treated with cycloheximide at different time points and exposed to normoxia or hypoxia ($n = 3$). (C) PASMCs were transfected with WT-GRK2 and HA-Ub plasmids and then exposed to normoxia or hypoxia pretreated with MG132. The proteins were immunoprecipitated with the antibody GRK2 and analyzed by Western blotting ($n = 3$). (D) Western blotting analysis of p-GRK2 at different sites in PASMCs stimulated with hypoxia at various time points ($n = 3$). $^{*}P < 0.05$ and $^{\dagger}P < 0.01$ *vs.* Ctl. The data represent the mean ± SEM. Ctl: Control; GAPDH: Glyceraldehyde 3-phosphate dehydrogenase; GRK2: G protein-coupled receptor kinase 2; HA-Ub: HA-tagged ubiquitin; IP: Immunoprecipitation; mRNA: Messenger Ribonucleic acid; NS: no statistical significance; PASMCs: Pulmonary arterial smooth muscle cells; p-GRK2: Phospho-G protein-coupled receptor kinase 2; SEM: Standard error of the mean; WT: Wild type.

followed by the treatment of the proteasomal inhibitor MG132. We found that hypoxia significantly decreased GRK2 ubiquitination levels by IP assay [Figure 7C]. The results suggest that hypoxia inhibits the ubiquitination degradation of GRK2.

A previous study reported that GRK2 phosphorylation at multiple sites may affect GRK2 activity in response to different stimuli.[23] Furthermore, one study reported that HEK-293 cells transfected with β-AR and GRK2 Y13 or Y86 or Y92F (Tyr-Phe) mutant markedly decreased GRK2 phosphorylation by c-Src in the presence of isoproterenol, which was particularly low in the Y13/86/92F triple mutant,[24] indicating mutation at Tyr86/13/92 sites blocking the GRK2 degradation by c-Src under β-AR activation. We therefore tested the impact of hypoxia on GRK2 phosphorylation at these sites. The GRK2 phosphorylation at Tyr13/92 did not significantly increase over time of hypoxia, whereas PASMCs exposed to 12–48 h hypoxia exhibited a consistent reduction in GRK2-Tyr 86 phosphorylation [Figure 7D]. Taken together, these findings suggest that GRK2 might be stabilized by inhibiting phosphorylating GRK2 on Tyr 86 and subsequently activating ubiquitylation under hypoxic conditions.

Discussion

The present study explores the importance of GRK2 in PAH development. We find that GRK2 has a critical role in PASMCs proliferation/migration in hypoxia plus SU5416-induced PH in mice and human PAH development through promoting YAP expression and nuclear translocation. Our findings should be very strongly clinically relevant. While the mechanisms of PAH are multi-factorial, excessive proliferation and migration of PASMCs in small pulmonary vessels, leading to medial thickening and luminal stenosis or occlusion with subsequent increased PVR and the phenotype of PAH, is the final common pathobiological mechanism of PAH. Our study presents four major findings. Increased levels of the GRK2 protein in most organs have been linked to many cardiovascular diseases;[6–10] however, the precise underlying mechanisms of GRK2 in the development of arterial hypertension are controversial,[10,25] as deletion of GRK2 in a mouse model did not prevent arterial hypertension development.[10] Here, we demonstrate that GRK2 protein levels positively correlate with PAH severity in patients and in mice with hypoxia-induced PAH, directly linking GRK2 signaling to PAH development. We further show that SMC-specific GRK2 knock-out mice are resistant to PAH development due to a decrease in vessel wall thickness and maintenance of the luminal area. Then, we show that GRK2 over-expression induces excessive PASMC proliferation and migration, mainly by increasing YAP protein expression and promoting YAP nuclear translocation. These findings described the importance of GRK2–YAP signaling in PAH development in both humans and mice.

Vasoconstriction and vascular remodeling of the pulmonary artery participate in PAH development and progression, from the beginning to the end stage of the disease.[1–6] Dysregulated pulmonary vascular control mediates and contributes to vascular remodeling[11,12,26] characterized by vasoconstriction, cellular hyperplasia, thrombosis, and sclerosis, resulting in luminal obliteration. This combination of features reduces pulmonary vascular

compliance. Gros *et al*[10] reported that GRK2 activity is selectively increased in lymphocytes from hypertensive subjects. Recently, Tutunea-Fatan *et al*[27] found that GRK2 expression is increased in arterial hypertension, facilitating the development of the hypertensive state by increasing the desensitization of GPCRs important for vasodilation. These researchers also reported that GRK2 deficiency leads to age-dependent development of hypertension as a consequence of global alterations in GPCR signaling, implying that the balance among mechanisms regulating vascular tone is shifted to favor vasoconstriction in the absence of GRK2 expression. Moreover, two studies highlighted the possible role of GRK2 in mediating pulmonary arterial relaxation upon exposure to blue light, with unknown mechanisms.[11,12] Our results demonstrate that the exaggerated pulmonary arterial remodeling in response to hypoxia can be mostly improved by specifically deleting GRK2 in PASMCs accompanied by inhibition of AKT phosphorylation—a known mediator of SMC proliferation.[22,28] These findings highlight the important roles and mechanisms of GRK2 in PAH development.

There is accumulating evidence for the importance of the HIPPO–YAP pathway in vascular remodeling and related cardiovascular diseases.[15,29] Consistently, our results show that YAP protein expression is significantly increased in the pulmonary artery of patients with PAH and in lung tissues of mice with hypoxia-induced PAH. Emerging evidence indicates a critical function for YAP in regulating PASMCs proliferation and migration and pulmonary vascular remodeling through an ECM–YAP feedback loop in animal models.[18,30] YAP has been implicated in the stiff matrix-induced expression of glutaminase attributed to PH.[31] In addition, LATS1, an upstream regulator of YAP, is inactivated in small pulmonary arterial VSMCs in PAH,[15,18,29] which induces the expression of its reciprocal effector YAP and increases fibronectin production and secretion by activating integrin-linked kinase 1 (ILK1) in pulmonary arterial VSMCs.[15] In turn, ILK1 negatively regulates LATS1, and this YAP–fibronectin–ILK1 signaling loop has been shown to control pulmonary arterial VSMC proliferation and survival. Therefore, a positive feedback loop involving actomyosin contractility, ECM stiffness, and sustained YAP activation contributes to hypoxia-induced PAH development at different levels.[15,29]

Nuclear YAP/TAZ mainly interacts with transcription factors of the TEAD family, and others, to regulate gene expression.[15,29–31] Upon phosphorylation by LATS1/2, YAP interacts with 14-3-3, which stabilizes YAP; in turn, YAP is prevented from translocating into the nucleus.[32] Here, our data point out that GRK2 promotes YAP translocation into the nucleus by increasing YAP expression and preventing the interaction of YAP with 14-3-3. Moreover, Moon *et al*[33] reported that Nemo-like kinase (NLK) phosphorylates YAP at Ser128 both *in vitro* and *in vivo*, which blocks interaction with 14-3-3 and enhances its nuclear localization. These studies have established that YAP inhibition via both LATS-dependent and LATS-independent mechanisms. We found that although LATS1 was down-regulated in response to hypoxia, LATS1 expression did not change in response to GRK2 over-expression, silencing, or deletion, indicating that the canonical HIPPO pathway is not modulated by GRK2. Furthermore, our data showed that GRK2 deletion inhibited YAP nuclear translocation, and that GRK2-YAP axis plays a crucial role in PAH development.

Our results show that hypoxia inhibits the ubiquitination degradation of GRK2. Enhanced GRK2 degradation by the proteasome pathway occurs upon GPCR stimulation, which allows cellular adaptation to chronic stimulation in a physiological setting.[7,23,24] ERK phosphorylation at Ser670 and S-nitrosothiol (SNO) at Ser340 inhibits GRK2 activation, while PKA phosphorylation at Ser 685 can promote GRK2 activation.[23] Conversely, GRK2 degradation under isoproterenol stimulation was diminished in cells transfected with β-AR and GRK2-Y13 or Y86 or Y92F mutant, which was particularly low in the Y13/86/92F triple mutant.[23,24] However, our results demonstrate that down-regulation of GRK2 ubiquitination levels by decreasing phosphorylating GRK2 at Tyr-86 (but not at Tyr-13 or Tyr-92) under hypoxia conditions. Conclusively, our findings reveal an effective way to regulate the rate of degradation of GRK2 and provide a potential therapeutic target for PAH.

It is essential to acknowledge the various constraints inherent in this study. To comprehensively assess the relationship between GRK2 expression and pulmonary artery pressure, as well as the severity of pulmonary vascular remodeling, further investigations with a larger sample size are warranted. In some respects, we encountered challenges in conclusively establishing YAP as the direct targets of GRK2. Furthermore, additional research efforts are imperative for a comprehensive understanding of the roles played by GRK2 in pulmonary vascular remodeling and for the development of innovative pharmaceutical interventions targeting GRK2 as a therapeutic strategy for pulmonary hypertension.

In summary, our results show that an increased baseline level of GRK2 protein correlates with increased PAH severity in both humans and mice under hypoxia. Despite pivotal studies have pointed out the YAP regulation by GPCR in heart development, regeneration, and disease,[34] we for the first show that the GRK2–YAP–AKT signaling pathway induces PASMCs proliferation and pulmonary vascular remodeling in response to hypoxia. These findings may be beneficial to provide effective strategies for the treatment of PAH.

Acknowledgement

We would like to thank Professor Zhongzhou Yang (Nanjing University) for providing the *Grk2*$^{f/f}$ mice strain (purchased from The Jackson Laboratory) used in this study.

Funding

This work was supported by a grant from the National Natural Scientific Foundation of China (Nos. NSFC 91639303 and NSFC 81770441).

Conflicts of interest

None.

References

1. Galie N, Humbert M, Vachiery JL, Gibbs S, Lang I, Torbicki A, *et al*. 2015 ESC/ERS Guidelines for the diagnosis and treatment of pulmonary hypertension: The Joint Task Force for the Diagnosis and Treatment of Pulmonary Hypertension of the European Society of Cardiology (ESC) and the European Respiratory Society (ERS): Endorsed by: Association for European Paediatric and Congenital Cardiology (AEPC), International Society for Heart and Lung Transplantation (ISHLT). Eur Heart J 2016;37:67–119. doi: 10.1093/eurheartj/ehv317.
2. Lau EMT, Giannoulatou E, Celermajer DS, Humbert M. Epidemiology and treatment of pulmonary arterial hypertension. Nat Rev Cardiol 2017;14:603–614. doi: 10.1038/nrcardio.2017.84.
3. Sitbon O, Sattler C, Bertoletti L, Savale L, Cottin V, Jais X, *et al*. Initial dual oral combination therapy in pulmonary arterial hypertension. Eur Respir J 2016;47:1727–1736. doi: 10.1183/13993003.02043-2015.
4. Lan NSH, Massam BD, Kulkarni SS, Lang CC. Pulmonary arterial hypertension: Pathophysiology and treatment. Diseases 2018;6:38. doi: 10.3390/diseases6020038.
5. Hussain MB, Marshall I. Characterization of alpha1-adrenoceptor subtypes mediating contractions to phenylephrine in rat thoracic aorta, mesenteric artery and pulmonary artery. Br J Pharmacol 1997;122:849–858. doi: 10.1038/sj.bjp.0701461.
6. Winstel R, Freund S, Krasel C, Hoppe E, Lohse MJ. Protein kinase cross-talk: Membrane targeting of the beta-adrenergic receptor kinase by protein kinase C. Proc Natl Acad Sci U S A 1996;93:2105–2109. doi: 10.1073/pnas.93.5.2105.
7. Penela P, Ribas C, Mayor F, Jr. Mechanisms of regulation of the expression and function of G protein-coupled receptor kinases. Cell Signal 2003;15:973–981. doi: 10.1016/s0898-6568(03)00099-8.
8. Wang Y, Gao E, Lau WB, Wang Y, Liu G, Li JJ, *et al*. G-protein-coupled receptor kinase 2-mediated desensitization of adiponectin receptor 1 in failing heart. Circulation 2015;131:1392–1404. doi: 10.1161/CIRCULATIONAHA.114.015248.
9. Yi XP, Gerdes AM, Li F. Myocyte redistribution of GRK2 and GRK5 in hypertensive, heart-failure-prone rats. Hypertension 2002;39:1058–1063. doi: 10.1161/01.hyp.0000019130.09167.3b.
10. Gros R, Benovic JL, Tan CM, Feldman RD. G-protein-coupled receptor kinase activity is increased in hypertension. J Clin Invest 1997;99:2087–2093. doi: 10.1172/JCI119381.
11. Sikka G, Hussmann GP, Pandey D, Cao S, Hori D, Park JT, *et al*. Melanopsin mediates light-dependent relaxation in blood vessels. Proc Natl Acad Sci U S A 2014;111:17977–17982. doi: 10.1073/pnas.1420258111.
12. Barreto Ortiz S, Hori D, Nomura Y, Yun X, Jiang H, Yong H, *et al*. Opsin 3 and 4 mediate light-induced pulmonary vasorelaxation that is potentiated by G protein-coupled receptor kinase 2 inhibition. Am J Physiol Lung Cell Mol Physiol 2018;14:L93–L106. doi: 10.1152/ajplung.00091.2017.
13. Piao L, Fang YH, Parikh KS, Ryan JJ, D'Souza KM, Theccanat T, *et al*. GRK2-mediated inhibition of adrenergic and dopaminergic signaling in right ventricular hypertrophy: Therapeutic implications in pulmonary hypertension. Circulation 2012;126:2859–2869. doi: 10.1161/CIRCULATIONAHA.112.109868.
14. Rodriguez-Serrano M, Rueda J, Buendia F, Monto F, Aguero J, Osa A, *et al*. beta2-Adrenoceptors and GRK2 as potential biomarkers in patients with chronic pulmonary regurgitation. Front Pharmacol 2019;10:93. doi: 10.3389/fphar.2019.00093.
15. Meng Z, Moroishi T, Guan KL. Mechanisms of Hippo pathway regulation. Genes Dev 2016;30:1–17. doi: 10.1101/gad.274027.115.
16. Yu FX, Zhao B, Panupinthu N, Jewell JL, Lian I, Wang LH, *et al*. Regulation of the Hippo-YAP pathway by G-protein-coupled receptor signaling. Cell 2012;150:780–791. doi: 10.1016/j.cell.2012.06.037.
17. Kudryashova TV, Goncharov DA, Pena A, Kelly N, Vanderpool R, Baust J, *et al*. HIPPO-integrin-linked kinase cross-talk controls self-sustaining proliferation and survival in pulmonary hypertension. Am J Respir Crit Care Med 2016;194:866–877. doi: 10.1164/rccm.201510-2003OC.
18. Dieffenbach PB, Haeger CM, Coronata AMF, Choi KM, Varelas X, Tschumperlin DJ, *et al*. Arterial stiffness induces remodeling phenotypes in pulmonary artery smooth muscle cells via YAP/TAZ-mediated repression of cyclooxygenase-2. Am J Physiol Lung Cell Mol Physiol 2017;313:L628–L647. doi: 10.1152/ajplung.00173.2017.
19. Li X, Zhang X, Leathers R, Makino A, Huang C, Parsa P, *et al*. Notch3 signaling promotes the development of pulmonary arterial hypertension. Nat Med 2009;15:1289–1297. doi: 10.1038/nm.2021.
20. Ma L, Yang F, Wu X, Mao C, Guo L, Miao T, *et al*. Structural basis and molecular mechanism of biased GPBAR signaling in regulating NSCLC cell growth via YAP activity. Proc Natl Acad Sci U S A 2022;119:e2117054119. doi: 10.1073/pnas.2117054119.
21. Luo J, Gu Y, Liu P, Jiang X, Yu W, Ye P, *et al*. Berberine attenuates pulmonary arterial hypertension via protein phosphatase 2A signaling pathway both in vivo and in vitro. J Cell Physiol 2018;233:9750–9762. doi: 10.1002/jcp.26940.
22. Tang H, Chen J, Fraidenburg DR, Song S, Sysol JR, Drennan AR, *et al*. Deficiency of Akt1, but not Akt2, attenuates the development of pulmonary hypertension. Am J Physiol Lung Cell Mol Physiol 2015;308:L208–L220. doi: 10.1152/ajplung.00242.2014.
23. Penela P. Chapter three – Ubiquitination and protein turnover of G-protein-coupled receptor kinases in GPCR signaling and cellular regulation. Prog Mol Biol Transl Sci 2016;141:85–140. doi: 10.1016/bs.pmbts.2016.04.002.
24. Penela P, Elorza A, Sarnago S, Mayor F, Jr. Beta-arrestin- and c-Src-dependent degradation of G-protein-coupled receptor kinase 2. EMBO J 2001;20:5129–5138. doi: 10.1093/emboj/20.18.5129.
25. Oyama JI, Node K. Is GRK2 a new target for cardiovascular disease? Hypertens Res 2018;41:575–577. doi: 10.1038/s41440-018-0052-2.
26. Pak O, Aldashev A, Welsh D, Peacock A. The effects of hypoxia on the cells of the pulmonary vasculature. Eur Respir J 2007;30:364–372. doi: 10.1183/09031936.00128706.
27. Tutunea-Fatan E, Caetano FA, Gros R, Ferguson SS. GRK2 targeted knock-down results in spontaneous hypertension, and altered vascular GPCR signaling. J Biol Chem 2015;290:5141–5155. doi: 10.1074/jbc.M114.615658.
28. Beaulieu JM, Sotnikova TD, Marion S, Lefkowitz RJ, Gainetdinov RR, Caron MG. An Akt/beta-arrestin 2/PP2A signaling complex mediates dopaminergic neurotransmission and behavior. Cell 2005;122:261–273. doi: 10.1016/j.cell.2005.05.012.
29. He J, Bao Q, Yan M, Liang J, Zhu Y, Wang C, *et al*. The role of Hippo/yes-associated protein signalling in vascular remodelling associated with cardiovascular disease. Br J Pharmacol 2018;175:1354–1361. doi: 10.1111/bph.13806.
30. Hoon JL, Tan MH, Koh CG. The regulation of cellular responses to mechanical cues by Rho GTPases. Cells 2016;5:17. doi: 10.3390/cells5020017.
31. Bertero T, Oldham WM, Cottrill KA, Pisano S, Vanderpool RR, Yu Q, *et al*. Vascular stiffness mechanoactivates YAP/TAZ-dependent glutaminolysis to drive pulmonary hypertension. J Clin Invest 2016;126:3313–3335. doi: 10.1172/JCI86387.
32. Dobrokhotov O, Samsonov M, Sokabe M, Hirata H. Mechanoregulation and pathology of YAP/TAZ via Hippo and non-Hippo mechanisms. Clin Transl Med 2018;7:23. doi: 10.1186/s40169-018-0202-9.
33. Moon S, Kim W, Kim S, Kim Y, Song Y, Bilousov O, *et al*. Phosphorylation by NLK inhibits YAP-14-3-3-interactions and induces its nuclear localization. EMBO Rep 2017;18:61–71. doi: 10.15252/embr.201642683.
34. Zhou Q, Li L, Zhao B, Guan KL. The hippo pathway in heart development, regeneration, and diseases. Circ Res 2015;116:1431–1447. doi: 10.1161/CIRCRESAHA.116.303311.

How to cite this article: Ye P, Deng YF, Gu Y, Liu PF, Luo J, Pu JQ, Chen JY, Huang Y, Wang NP, Ji Y, Chen SL. GRK2–YAP signaling is implicated in pulmonary arterial hypertension development. Chin Med J 2024;137:846–858. doi: 10.1097/CM9.0000000000002946